EFFECT OF INTERPLANETARY SHOCKS AND MAGNETIC CLOUDS ON ONSET OF COSMIC-RAY DECREASES

A. G. ANANTH* and D. VENKATESAN

Institute for Space Research Department of Physics and Astronomy, The University of Calgary, Calgary, Alberta, T2N 1N4 Canada

(Received 19 March, 1992; in revised form 13 August, 1992)

Abstract. A detailed analysis has been carried out to study the onset times of cosmic-ray decreases occurring during 1978–1982 with respect to the arrival times of interplanetary shocks and magnetic clouds. The observations demonstrate that shocks, magnetic clouds and a combination of both could effectively trigger a cosmic-ray decrease when they are associated with turbulent sheaths of maximum thickness ≤ 15.0 hr (≤ 0.15 AU). Further, the shocks associated with enhanced solar wind velocity produce a fast decrease and the magnetic clouds accompanied by extended and enhanced magnetic field produce a slow decrease. The decrease, non-correlated with the arrival times of shocks and magnetic clouds, represents a corotating cosmic-ray decrease produced by corotating streams.

1. Introduction

The study of cosmic-ray (CR) decreases has assumed a rather significant importance in determining interplanetary field and flow configurations. Further, it has been found that the decreases are mostly caused by interplanetary transients originating from solar flares (Burlaga, 1983) and corotating high-speed streams originating from solar coronal holes on the Sun (Venkatesan, Shukla, and Agrawal, 1982). A major problem has been the identification of field and flow configurations and physical mechanisms causing cosmic ray modulation. Barouch and Burlaga (1975) have shown that such decreases are sometimes associated with magnetic field enhancements. The perpendicular gradient drifts in the high magnetic field region have been suggested as mostly responsible for these decreases (Sarris, Dodopoulos, and Venkatesan, 1989, Cheng, Sarris, and Dodopoulos, 1990).

The identification of interplanetary shocks associated with magnetic clouds (Burlaga *et al.*, 1981; Klein and Burlaga, 1982) have provided a new tool for investigating the physical process responsible for CR decreases. Using the superposed epoch analysis technique for a number of events, Badruddin, Yadav, and Yadav (1986), Badruddin, Venkatesan, and Zhu (1991), and Zhang and Burlaga (1988) have demonstrated that the decreases are essentially produced by the turbulent sheath between the interplanetary shock and the magnetic cloud. It has also been shown that the post-shock turbulent region is more effective in producing the main phase of CR decreases than an enhanced, ordered magnetic field (Nishida, 1982; Chih and Lee, 1986; Webb and Wright, 1990). Lockwood, Webber, and Debrunner (1991), by considering only Forbush decreases

* Permanent address: Indian Space Research Organization, Department of Space, New BEL Road, Bangalore, India.

Solar Physics **143:** 373–383, 1993.

associated with shock and magnetic clouds, arrived at the conclusion that magnetic clouds are not very effective in producing the main phase of a Forbush decrease.

Sanderson *et al.* (1990a, b) using the magnetic cloud data of Marsden *et al.* (1987) have clearly shown that CR decreases are also produced by magnetic clouds. They have suggested that post-shock regions, tangential discontinuities and magnetic clouds are equally effective in producing CR decreases. Kahler and Reames (1991), considering magnetic fields of different topology, have suggested that the CR decreases could also be produced by the passage of magnetic clouds with open field-line configurations.

The earlier investigations indicated different mechanisms for the production of CR decreases. Hence, we need to determine the most appropriate physical mechanisms and the interplanetary configuration responsible for the CR decreases. By considering each individual event, we have examined in great detail different types of CR decreases (not necessarily Forbush decreases) associated with shocks and magnetic clouds. We have also derived the interplanetary plasma and magnetic field parameters for a different category of events classified on the basis of CR decrease profiles observed with respect to the arrival times of shocks and magnetic clouds. The results are presented and discussed in this paper.

2. Data Analysis

We have considered all available magnetic cloud events (Klein and Burlaga, 1982; Zhang and Burlaga, 1988) for the period 1967–1982. For each event we have determined the arrival time of the shock by identifying the geomagnetic Sudden Storm Commencement (SSC) as derived in Badruddin, Venkatesan, and Zhu (1991). It is considered more appropriate than the satellite data (Lockwood, Webber, and Debrunner, 1991), since we observe CR decreases at the Earth. Further, we have selected only events where the magnetic clouds are followed by the arrival of a shock front at the Earth. We note that only the magnetic cloud events of Zhang and Burlaga (1988) meet the specific selection criteria that the SSC (shock) should occur before the arrival of the magnetic cloud. We have identified for each event a CR decrease recorded by the super neutron monitor at Calgary (lat. 51.05° N, long. 114.08° W, cut-off rigidity 1.09 GV) occurring within a few hours (< 3 hr) of the arrival of shocks and magnetic clouds. Since most of the events exhibit isotropic, cosmic-ray decreases, we have used data from only one station (Calgary) for determining the decrease profiles. The 16 events selected for our analysis are listed in Table I along with the shock arrival times as determined by SSC, the arrival times of magnetic clouds as determined from satellite data (Zhang and Burlaga, 1988), onset times of the CR decreases, times of minimum intensity and the amplitudes of the decreases.

A careful examination of Table I indicates that the events can be broadly divided into four categories based on the onset times of the CR decreases. Category 1 events show that the onset of the CR decrease coincides with the arrival time of the shock front (< 2 hr). Category 2 shows that the CR decrease starts only at the arrival of the magnetic cloud (< 3 hr). Category 3 reveals that the onset of the cosmic-ray decrease

TABLE I

A detailed list of the cosmic-ray decrease events selected for the present analysis. The arrival time of the shock front, magnetic cloud, the onset time of the cosmic-ray decrease, time of minimum cosmic-ray intensity time delay $\Delta = (Ts - Tm)$, amplitude of the cosmic-ray decrease, and the category of each event are given. The asterisk (*) indicates the onset time of the cosmic-ray decrease with respect to the arrival time of the shock front and magnetic cloud.

No.	Event	Shock arrival time (Ts) (SSC onset)		Magnetic cloud arrival time (Tm)		Cosmic-ray decrease onset time		Cosmic ray intensity minimum		Time delay $\Delta = Ts - Tm$ (hr)	Amp. of decrease (%)	Cat. No.
		Date	Time UT (hr)	Date	Time UT (hr)	Date	Time UT (hr)	Date	Time UT (hr)			
1	10 Feb. 1969	10 Feb.	20:24*	11 Feb.	09:00	10 Feb.	20:00*	11 Feb.	09:00	12.6	3.0	1
2	29 Sep. 1978	29 Sep.	03:01*	29 Sep.	10:00	29 Sep.	01:00*	29 Sep.	07:00	6.9	6.8	1
3	29 Oct. 1978	29 Oct.	11:16*	29 Oct.	23:00	29 Oct.	11:00*	29 Oct.	14:00	11.7	1.0	1
4	11 Dec. 1980	11 Dec.	10:09*	11 Dec.	23:00	11 Dec.	09:00*	12 Dec.	00:00	12.8	3.0	1
5	3 Apr. 1979	3 Apr.	10:01	3 Apr.	22:00*	3 Apr.	23:00*	4 Apr.	06:00	11.9	3.6	2
6	19 Mar. 1980	19 Mar.	06:17	19 Mar.	16:00*	19 Mar.	17:00*	20 Mar.	06:00	9.7	4.2	2
7	6 Feb. 1981	6 Feb.	08:47	6 Feb.	19:00*	6 Feb.	19:00*	7 Feb.	06:00	10.2	2.3	2
8	11 Feb. 1982	11 Feb.	13:13	12 Feb.	03:00*	12 Feb.	00:00*	12 Feb.	06:00	13.8	5.0	2
9	3 Jan. 1978	3 Jan.	20:42*	4 Jan.	12:00	3 Jan.	21:00*	4 Jan.	16:00	15.3	6.8	3
10	27 Aug. 1978	27 Aug.	02:46*	27 Aug.	18:00	27 Aug.	00:00*	27 Aug.	23:00	15.2	3.0	3
11	19 Dec. 1980	19 Dec.	04:56*	19 Dec.	14:00	19 Dec.	05:00*	19 Dec.	19:00	9.1	6.1	3
12	25 Sep. 1982	25 Sep.	20:30*	25 Sep.	22:00	25 Sep.	20:00*	26 Sep.	02:00	1.5	2.0	3
13	4 June 1978	4 June	12:11	5 June	00:00	4 June	19:00	4 June	23:00	11.8	1.6	4
14	15 Feb. 1980	15 Feb.	12:35	16 Feb.	04:00	15 Feb.	16:00	16 Feb.	02:00	15.4	1.6	4
15	5 Mar. 1981	5 Mar.	05:35	5 Mar.	13:00	5 Mar.	20:00	6 Mar.	04:00	7.4	4.0	4
16	19 Sep. 1981	19 Sep.	01:37	19 Sep.	07:00	18 Sep.	18:00	19 Sep.	06:00	5.4	2.5	4

starts immediately with the shock arrival (< 2 hr) and continues even after the magnetic cloud arrival. Both categories 2 and 3 indicate cosmic-ray minima a few hours after the arrival of a magnetic cloud. Category 4 shows that the onset of the CR decrease is not associated with either the shock arrival or magnetic cloud. Further we estimate from Table I the maximum time delay (Δ) between the arrival time of the shock (Ts) and the magnetic clouds (Tm) as $\Delta = Ts - Tm \leq 15$ hr.

3. Results and Discussion

Figure 1 shows typical examples of the four categories of events listed in Table I. The arrival times of shocks (solid line) and magnetic clouds (dotted line) as observed for the

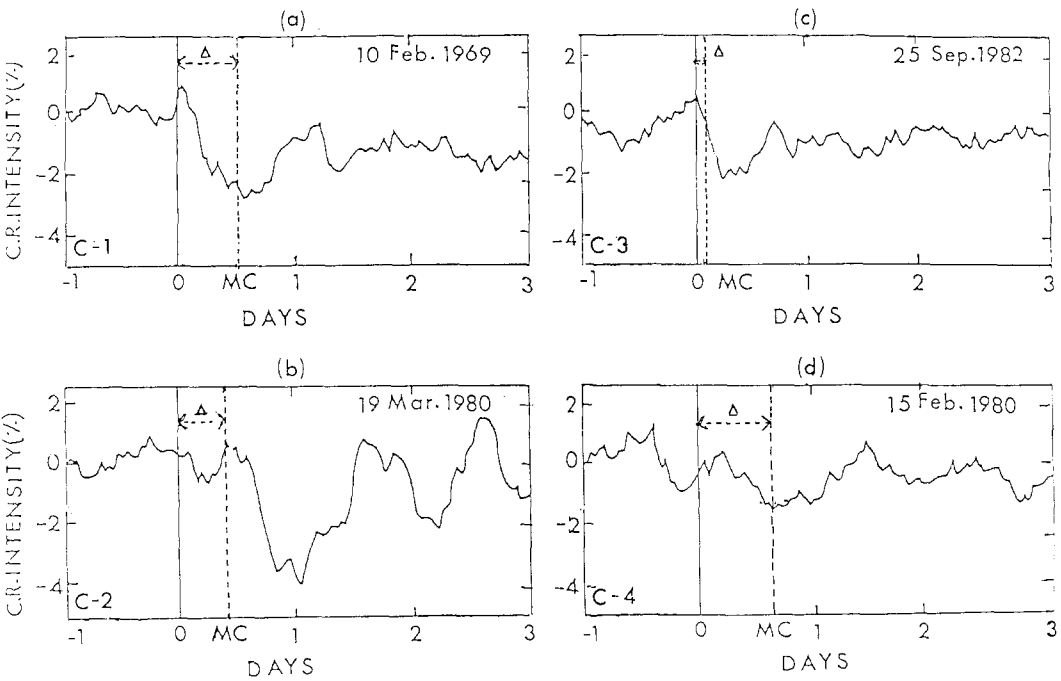

Fig. 1. Typical examples of cosmic-ray decrease profiles for the four categories of events initiated by (a) shock front, (b) magnetic cloud, (c) combination of shock and magnetic cloud and, (d) corotating streams. The arrival times of a shock (thin line) and those of magnetic clouds (dotted lines) observed for the event are also marked therein.

events are also indicated in the same figure. Figure 1(a) clearly illustrates that the CR decrease for Category 1 starts immediately following the shock arrival and is completed before the arrival of the magnetic cloud. Thus it is seen that the decrease is mainly triggered by the arrival of the shock front. For Category 2 (Figure 1(b)), the CR decrease starts only with the arrival of the magnetic cloud and continues for a long time. We therefore conclude that these events are essentially produced by the arrival of the magnetic clouds. In the case of Category 3, we note that the CR decrease starts

immediately after the arrival of the shock (Figure 1(c)), but continues to decrease even after the arrival of the magnetic cloud. Thus, in this case both the shocks and magnetic clouds are associated with producing the CR decrease. Category 4 shows a different type of CR decrease profile (Figure 1(d)). Here we find that the onset of the CR decrease is not associated with either the arrival of the shock or the magnetic cloud. The decrease in this case resembles a corotating type of CR decrease. Thus, the examples of the individual events (shown in Figure 1 and Table I) clearly demonstrate that the CR decrease could be caused by either the arrival of a shock, a magnetic cloud or a combination of both. The corotating CR decreases do not reveal any correlation with the arrival of the shock or the magnetic cloud and appear to be produced by a different mechanism.

In order to derive the interplanetary configurations associated with the four categories of CR decreases, we have subjected hourly cosmic-ray data and the interplanetary field and plasma data (derived from satellites, IMP-8 and ISEE-3) recorded for each individual event to superposed epoch (Chree) analysis. The zero epoch is chosen either as the arrival time of the shock or that of the magnetic cloud (as appropriate to each category). Since the superposed epoch analysis could be carried out with only one epoch for the zero hour, we represent the other epoch by the maximum delay time ($\Delta \sim 15$ hours) estimated from Table I. Further, we have derived the average CR profiles and interplanetary characteristics for each category by superposed epoch analysis of individual events listed under that category. The CR intensity deviations, interplanetary magnetic field and solar wind parameters derived for each category are plotted and shown in Figures 2, 3, 4, and 5. In all these figures, the dotted lines indicate the other epoch computed by the maximum time delay $\Delta \approx 15$ hr. The errors associated with cosmic-ray intensity derived from count rates are also marked in the figures. It may be noted here that the CR decrease profiles given in earlier papers are essentially derived by combining all the events and subjecting them to superposed epoch analysis without considering the behaviour of individual events with respect to the time of arrival of shocks and magnetic clouds.

For the first category, Figure 2 shows the CR intensity variation, interplanetary magnetic field intensity, field fluctuations, and plasma velocity as a function of time based on the shock arrival time of the shock (as the zero epoch hour). It is evident from the figure that the CR decrease is triggered by the passage of the shock. The cosmic-ray intensity reaches a minimum amplitude ($\sim 3.0\%$) in a time interval of ~ 15 hr and before the arrival of the magnetic cloud. The figure also reveals that the magnetic field fluctuations (σF) following the shock front are considerably larger than the normal values. This indicates the presence of a turbulent sheath between the shock front and the magnetic cloud. Thus the observations show that the CR decrease in this case is effectively produced by the turbulant sheath between the shock and the magnetic cloud. These observations further confirm the conclusions of Zhang and Burlaga (1988), Badruddin, Venkatesan, and Zhu (1991) and Lockwood, Webber, and Debrunner (1991) that the post-shock turbulent region is more effective in producing the CR decreases. It can also be seen from the figure that for these events the solar wind velocity

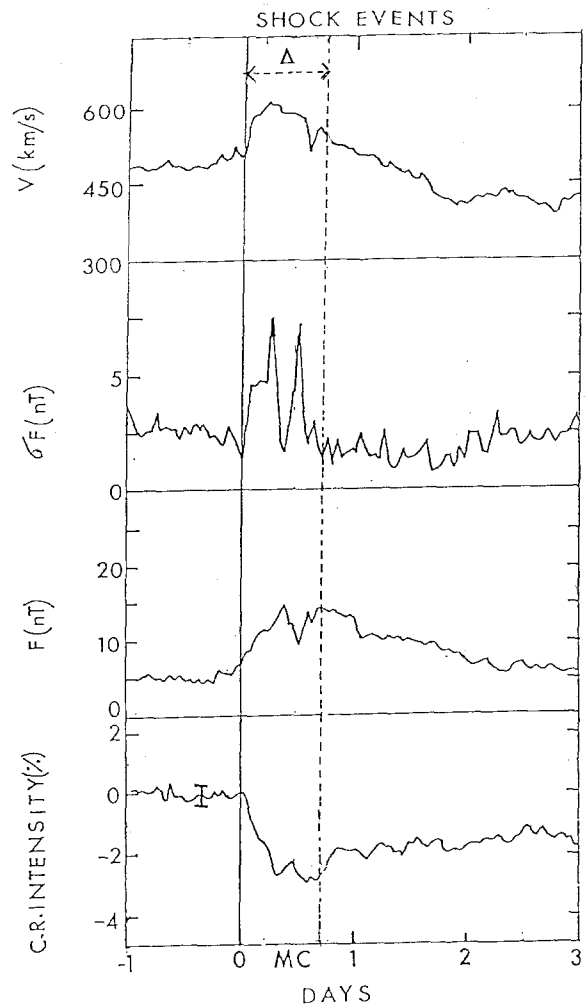

Fig. 2. The cosmic-ray intensity decrease plotted for Category 1 events along with the interplanetary magnetic field (F), field fluctuations (σF), solar wind velocity (V) derived using the arrival time of the shock as zero epoch hour. Note that the cosmic-ray decrease starts with the arrival of the shock front.

following the shock front is higher (~ 600 km s^{-1}) than the solar wind velocity before the shock. The interplanetary magnetic field (~ 12 nT) associated with the CR decrease is comparable with the magnetic field normally observed during the passage of a shock front associated with a magnetic cloud. The observations clearly show that the shock-initiated events are associated with a fast CR decrease profile and enhanced solar wind velocity.

For Category 2, we use the arrival times of the magnetic cloud as zero epoch; CR variations for these events are shown in Figure 3. Note that here the decrease starts just before the arrival of the magnetic cloud and decreases gradually to reach a minimum intensity level ($\sim 3\%$) nearly 20 hr after the passage of the magnetic cloud. These

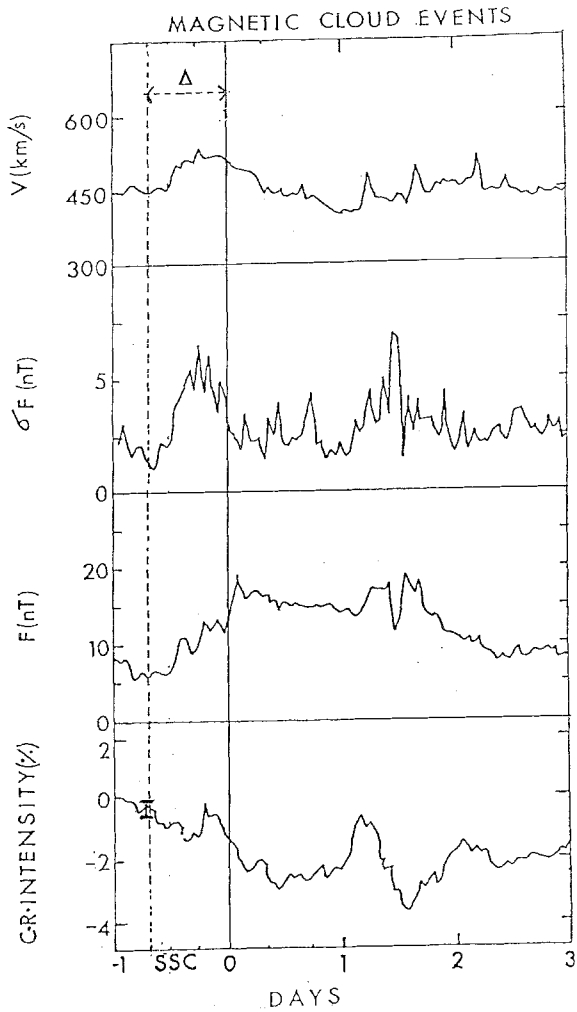

Fig. 3. The cosmic ray intensity decrease plotted for Category 2 events along with the interplanetary magnetic field (B), field fluctuations (σF), and solar wind velocity (V) derived from using the arrival time of the magnetic cloud as the zero-epoch hour. Note that the slow cosmic-ray decrease starts with the arrival of the magnetic clouds.

observations suggest that the CR decrease is essentially triggered by the passage of a magnetic cloud. Our observations agree with the observations of Sanderson *et al.* (1991) and Kahler and Reames (1991) that the magnetic clouds are also effective in producing CR decreases. Further we note that in the case of Category 2 events, the magnetic field strength following the arrival of the magnetic cloud increases rapidly to ~ 20 nT and remains high (~ 15 nT) for a considerable length of time (~ 24 hr). This suggests that the magnetic clouds producing the CR decrease are associated with enhanced and extended magnetic fields. The magnetic field fluctuations (σF) following the passage of the shock front are high, indicating that even for Category 2 the post-shock region is

turbulent. The solar wind velocity does not show any large enhancement in comparison to Category 1 during the passage of the shock or the magnetic cloud. The observations thus clearly show that the CR decrease for Category 2 events exhibits a slow decrease profile following the arrival of the magnetic cloud associated with an enhanced and extended magnetic field region.

Figure 4 shows, for Category 3, CR variation and all other parameters with the arrival time of the shock as zero epoch. Note here that the CR decrease starts immediately after the shock arrival and reaches a minimum intensity ($\sim 3\%$) nearly 12 hours after the arrival of the shock and remains depressed for < 3 hr even after the arrival of the

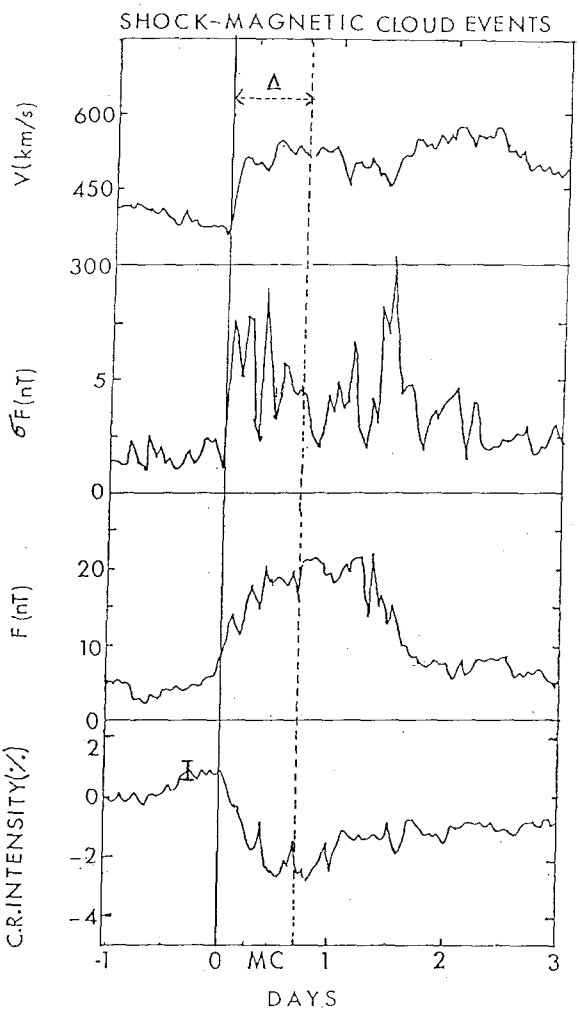

Fig. 4. The cosmic-ray intensity decrease plotted for Category 4 events along with the interplanetary magnetic field (B), field fluctuations (σF), and solar wind velocity (V) derived using the arrival time of the shock as the zero-epoch hour. Note that the cosmic-ray decrease starts with the arrival of the shock front and remains depressed even after the arrival of the magnetic cloud.

magnetic cloud. It can be further seen from the figure that the magnetic cloud is associated with enhanced magnetic field (~ 20 nT) extending over a period of nearly 24 hr. We also find that for these events, the magnetic clouds are associated with enhanced plasma velocity (~ 500 km s^{-1}) and field fluctuations (σF). The observations reveal that the CR decreases for Category 3 events are caused by a combination of both shocks and magnetic clouds, and the magnetic clouds in this case are associated with an extended region of enhanced interplanetary field. We find that even in the case of Category 3, the field fluctuations following the passage of the shock front remain enhanced, indicating the presence of a post-shock turbulent region.

Figure 5 refers to Category 4 which again uses the shock arrival time of the shock

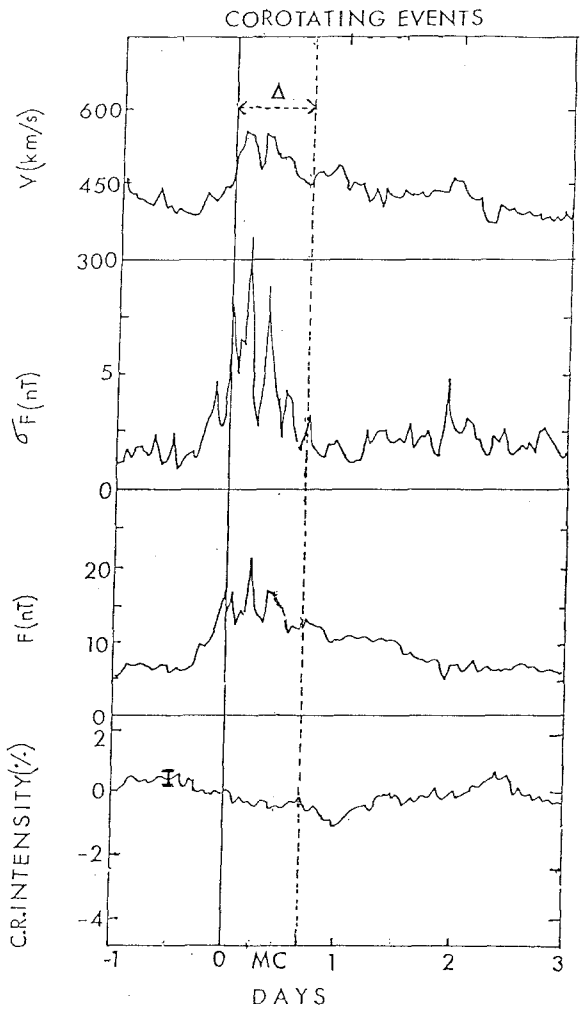

Fig. 5. The cosmic-ray intensity decreases plotted for Category 4 events along with the interplanetary magnetic field (B), field fluctuations (σF), solar wind velocity (V) derived using the arrival time of the shock as zero epoch hour. Note that the onset of a corotating cosmic-ray decrease is not correlated with the arrival of a shock front or magnetic cloud.

as zero epoch. We find that the CR decrease in this case is quite small ($\sim 1\%$), and it is neither correlated with the arrival time of the shock front nor with that of the magnetic cloud. The decrease profile is similar to that of a corotating CR decrease normally produced by corotating streams (Burlaga, 1983). Further, the figure does not show the presence of an enhanced and extended magnetic cloud region, as we have observed in Categories 2 and 3. The interplanetary parameters observed in the figure for Category 4 are consistent with the passage of shocks and magnetic clouds. Note however, that the magnetic field fluctuations (σF) associated with the post-shock region are very much enhanced, indicating the presence of a turbulent sheath following the passage of the shock. It emerges that corotating CR decreases are not triggered by the arrival of shocks and magnetic clouds. The CR decrease in this case is small and essentially caused by a mechanism which is quite different from the other three categories. The significance of the effect of interplanetary plasma and magnetic field on producing a corotating CR decrease has been studied by Barouch and Burlaga (1975) and Sarris, Dodopoulos, and Venkatesan (1989).

The observations presented clearly show that the shock-triggered events have a fast CR decrease profile associated with an enhanced plasma velocity. The magnetic-cloud triggered events have a slow CR decrease profile associated with an enhanced and extended magnetic field region. The events produced by the combination of shock and magnetic clouds indicate enhancement in both magnetic field and solar wind parameters. All of the three categories of events show a well-defined large CR decrease and are associated with enhanced interplanetary conditions. These observations would clearly suggests that the CR decrease for Categories 1, 2, and 3 are caused by interplanetary transients (Burlaga, 1983) produced by solar flare effects. However, we find for Category 4 that the CR decrease is neither triggered by the arrival of the shock front or that of the magnetic cloud, and the solar wind and magnetic field parameters are not very much enhanced as observed in the case of the other three categories. The CR decrease associated with Category 4 is small, $\sim 1\%$, and resembles a corotating type of decrease. Such decreases can only be attributed to the corotating streams produced by solar coronal holes (Hundhausen, 1977; Burlaga and King, 1979). CR decreases in such cases are normally produced by the gradient drift of particles (Barouch and Burlaga, 1976). It is important to note that for all the four categories, the CR decreases are associated with the presence of a turbulent sheath and they play a very significant role in producing a CR decrease.

We also observe that the sheath thickness determined by the maximum time delay between the arrival of the shock and the magnetic cloud is less than ≤ 15 hr. This would indicate that the thickness of the cosmic-ray modulating region is ≤ 0.15 AU, if we assume a normal solar wind speed of ~ 400 km s^{-1}. This is consistent with the sheath thickness determined by Lockwood, Webber, and Debrunner (1991).

4. Conclusions

From the above results we make the following conclusions:

(1) A fast CR decrease is produced by the passage of a shock front associated with an enhanced turbulence sheath.

(2) A slow CR decrease is produced by the passage of a magnetic cloud associated with an enhanced and extended magnetic field region.

(3) A CR decrease is also produced by the combination of a shock and a magnetic cloud when they are associated with an enhanced and extended field region.

(4) The corotating CR decrease could be produced by the corotating streams associated with shocks and magnetic clouds, but neither of them play any significant role in triggering the decrease.

(5) A CR decrease is always observed to be associated with an effective turbulent sheath region having a maximum thickness of $\Delta \leq 0.15$ AU.

Acknowledgement

A. G. Ananth is thankful for the award of a Visiting Fellowship under NSERC Grant to D. Venkatesan during which period the work was done. The authors are thankful to Suresh Pillai for computational assistance.

References

Badruddin, Yadav, R. S., and Yadav, N. R.: 1986, *Solar Phys.* **105**, 413.
Badruddin, Venkatesan, D., and Zhu, B. Y.: 1991, *Solar Phys.* **134**, 203.
Barouch, E. and Burlaga, L. F.: 1975, *J. Geophys. Res.* **80**, 449.
Barouch, E. and Burlaga, L. F.: 1976, *J. Geophys. Res.* **81**, 2103.
Burlaga, L. F.: 1983, *18th Int. Cosmic Ray Conf., Bangalore* **12**, 21.
Burlaga, L. F. and King, J.: 1979, *J. Geophys. Res.* **84**, 6633.
Burlaga, L. F., Sittler, E., Mariani, F., and Schwenn, R.: 1981, *J. Geophys. Res.* **86**, 6673.
Cheng, A. F., Sarris, E. T., and Dodopoulos, C.: 1990, *Astrophys. J.* **350**, 413.
Chih, P. P. and Lee, M. A.: 1986, *J. Geophys. Res.* **91**, 2903.
Hundhausen, A. J.: 1977, *Coronal Holes and High Speed Streams*, Boulder, 2908.
Klein, L. W. and Burlaga, L. F.: 1982, *J. Geophys. Res.* **87**, 613.
Lockwood, J. A., Webber, W. R., and Debrunner, H.: 1991, *J. Geophys. Res.* **96**, 11587.
Marsden, R. G., Sanderson, T. R., Tranquille, C., Wenzel, K. P., and Smith, E. J.: 1987, *J. Geophys. Res.* **92**, 11009.
Nishida, A.: 1982, *J. Geophys. Res.* **87**, 6003.
Sanderson, T. R., Beeck, J., Marsden, R. G., Tranquille, C., Wenzel, K. P., McKibben, R. B., and Smith, E. J.: 1990a, *21st Int. Cosmic Ray Conf., Adelaide* **6**, 251.
Sanderson, T. R., Beeck, J., Marsden, R. G., Tranquille, C., Wenzel, K. P., McKibben, R. B., and Smith, E. J.: 1990b, *21st Int. Cosmic Ray Conf., Adelaide* **6**, 255.
Sarris, E. T., Dodopoulos, C. A., and Venkatesan, D.: 1989, *Solar Phys.* **120**, 153.
Venkatesan, D., Shukla, A. K., and Agrawal, S. P.: 1982, *Solar Phys.* **81**, 375.
Webb, D. F. and Wright, C. S.: 1990, *21st Int. Cosmic Ray Conf., Adelaide* **6**, 213.
Zhang, G. and Burlaga, L. F.: 1988, *J. Geophys. Res.* **93**, 2511.